# Cascades and statistical equilibrium in shell models of turbulence

P. D. Ditlevsen and I. A. Mogensen

*The Niels Bohr Institute, Department for Geophysics, University of Copenhagen, Juliane Maries Vej 30,*

*DK-2100 Copenhagen Ø, Denmark*

We study the Gledzer-Okhitani-Yamada shell model simulating the cascade processes of turbulent flow. The model has two inviscid invariants governing the dynamical behavior. Depending on the choice of interaction coefficients, or coupling parameters, the two invariants are either both positive definite, analogous to energy and enstrophy of two-dimensional (2D) flow, or only one is positive definite and the other not, analogous to energy and helicity of 3D flow. In the 2D-like model the dynamics depend on the spectral ratio of enstrophy to energy. That ratio depends on wave number as $k^{\alpha}$. The enstrophy transfer through the inertial subrange can be described as a forward cascade for $\alpha < 2$ and diffusion in a statistical equilibrium for $\alpha > 2$. The $\alpha = 2$ case, corresponding to 2D turbulence, is a borderline between the two descriptions. The difference can be understood in terms of the ratio of typical time scales in the inertial subrange and in the viscous subrange. The multifractality of the enstrophy dissipation also depends on the parameter $\alpha$ and seems to be related to the ratio of typical time scales of the different shell velocities.

PACS number(s): 47.27.−i

## I. INTRODUCTION

The standard Kolmogorov $k^{-5/3}$ scaling law for energy cascading in three-dimensional (3D) turbulence and the corresponding $k^{-3}$ scaling law for enstrophy cascade in 2D turbulence is still debated. Direct numerical calculations of the full Navier-Stokes equation is by and large still impossible for high Reynolds number ($>100-200$) flows. However, the cascading mechanisms and its multifractal nature can be analyzed in reduced wave-number models for very high Reynold numbers with high accuracy. In this paper we investigate the Gledzer-Okhitani-Yamada (GOY) shell model [1,2], where the spectral velocity or vorticity is represented by one complex variable for each shell evenly spaced in $\log(k)$ in spectral space. For this type of model the Kolmogorov scaling arguments can be applied as for real flow regardless of how realistically they mimic the dynamics of the Navier-Stokes equation. The scaling behavior of the fields depends on the inviscid invariants of the model. In the simple model we are able to control which symmetries and conserved integrals of the dynamics are present in the inviscid and force-free limit. In the models we interpret as simulating 3D turbulence there are two inviscid invariants, similar to energy and helicity [3], of which the first is positive definite and the second is not. For the models we interpret as 2D turbulence the two inviscid invariants, similar to energy and enstrophy, are both positive definite. We will mainly be concerned with an investigation of the 2D-like models. The specific parameter choice previously assigned to simulating 2D turbulence is such that the GOY model does not show enstrophy cas-

cading but rather a statistical equilibrium where the enstrophy is transported through the inertial subrange by diffusion [4]. We show that this is a borderline case for which, on one side, the model behaves as a cascade model and, on the other side, it behaves as a statistical equilibrium model, where the enstrophy spectrum is characterized by a simple equipartitioning among the degrees of freedom of the model. The difference in behavior is connected with the different typical time scales of the shell velocities as a function of shell number. This probably also influences the (nonuniversal) multifractal behavior of the shell velocities. If time scales in the viscous subrange are not smaller than in the beginning of the inertial subrange, the low-wave-number end, the model does not have a multifractal spectrum.

## II. THE GOY MODEL

The GOY model is a simplified analogy to the spectral Navier-Stokes equation for turbulence. The spectral domain is represented as shells, each of which is defined by a wave number $k_n = k_0 \lambda^n$, where $\lambda$ is a scaling parameter defining the shell spacing; in our calculations we use the standard value $\lambda = 2$. The reduced phase space enables us to cover a large range of wave numbers, corresponding to large Reynolds numbers. We have $2N$ degrees of freedom, where $N$ is the number of shells, namely, the generalized complex shell velocities or vorticities, $u_n$ for $n = 1, N$. The dynamical equation for the shell velocities is

$$\dot{u}_n = ik_n\left(au_{n+2}^{*}u_{n+1}^{*} + \frac{b}{\lambda}u_{n+1}^{*}u_{n-1}^{*} + \frac{c}{\lambda^2}u_{n-1}^{*}u_{n-2}^{*}\right) - \nu k_n^{p_1}u_n - \nu' k_n^{-p_2}u_n + f_n, \tag{1}$$

where the first term represents the nonlinear wave interaction or advection, the second term is the dissipation, the third term is a drag term, specific to the 2D case, and the fourth term is the forcing. Boundary conditions at the two ends of the spectrum are simply $u_{-1} = u_0 = u_{N+1} = u_{N+2} = 0$. Throughout this paper we use $p_1 = p_2 = 2$. We will for convenience set $a = k_0 = 1$, which can be done in (1) by a rescaling of time and the units in $k$ space. A real form of the GOY model, as originally proposed by Gledzer [1], can be obtained trivially by having purely imaginary velocities and forcing. The GOY model in its original real form contains no information about phases between waves, thus a flow field in real space cannot be assigned to the spectral field. The complex form of the GOY model and extensions in which there are more shell variables in each shell introduce some degrees of freedom, which could be thought of as representing the phases among waves. However, it seems as if these models do not behave differently from the real form of the model in regard to the conclusions in the following [5,4]. The key issue for the behavior of the model is the symmetries and conservation laws obeyed by the model.

### A. Conservation laws

The GOY model has two conserved integrals, in the case of no forcing and no dissipation ($\nu = f = 0$). We denote the two conserved integrals by

$$E^{1,2} = \sum_{n=1}^{N} E_n^{1,2} = \frac{1}{2} \sum_{n=1}^{N} k_n^{\alpha_{1,2}} |u_n|^2 = \frac{1}{2} \sum_{n=1}^{N} \lambda^{n\alpha_{1,2}} |u_n|^2. \quad (2)$$

By setting $\dot{E}^{1,2} = 0$ and using $\dot{u}_n$ from (1) we get

$$1 + bz_1 + cz_1^2 = 0,$$
$$1 + bz_2 + cz_2^2 = 0, \quad (3)$$

where the roots $z_{1,2} = \lambda^{\alpha_{1,2}}$ are the generators of the conserved integrals. In the case of negative values of $z$ we can use the complex formulation $\alpha = (\ln|z| + i\pi)/\ln\lambda$. The parameters $b$ and $c$ are determined from (3) as

$$b = -(z_1 + z_2)/z_1 z_2,$$
$$c = 1/z_1 z_2. \quad (4)$$

In the $(b,c)$ parameter plane the curve $c = b^2/4$ represents models with only one conserved integral; see Fig. 1. Above the parabola the generators are complex conjugates and below they are real and different. Any conserved integral represented by a real nonzero generator $z$ defines a line in the $(b,c)$ parameter plane, which is tangent to the parabola in the point $(b,c) = (-2/z, 1/z^2)$. The rest of our analysis we will focus on the line defined by $z_1 = 1$. The conserved integral

$$E^1 = \frac{1}{2} \sum_{n=1}^{N} |u_n|^2 \quad (5)$$

is the usual definition of the energy for the GOY model [3]. The parameters are then determined by $1 + b + c = 0$, which with the definitions $b = -\epsilon$ and $c = -(1-\epsilon)$ agree with the
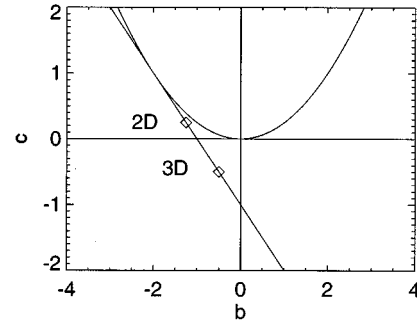


FIG. 1. $(b,c)$ parameter space. The model has two conserved integrals $E^{1,2} = 1/2\Sigma z_{1,2}^n |u_n|^2$. Above the parabola $z_1$ and $z_2$ are complex conjugates, on the parabola $z_1 = z_2$, and below $z_1$ and $z_2$ are real and different. Any real $z$ defines a line tangent to the parabola. The line drawn indicates where the one conserved integral is the energy, defined as $E = \frac{1}{2}\Sigma|u_n|^2$ ($z_1 = 1$). For $c>0$ the second conserved integral is positive definite ($z_2>0$), so the models are 2D-like. For $c<0$ this is not the case ($z_2<0$) and the models are 3D-like. The case $c=0$ is singular ($z_2 = \infty$), corresponding to $E^2 = |u_N|^2$. The diamonds indicate the standard 2D and 3D GOY models.

notation of Ref. [6]. The generator of the other conserved integral is $z_2 = 1/(\epsilon - 1)$, so for $\epsilon < 1$ the second conserved integral is not positive definite and of the form

$$E^2 = H = \frac{1}{2} \sum_{n=1}^{N} (-1)^n |z_2|^n |u_n|^2, \quad (6)$$

which can be interpreted as a generalized helicity. For $\epsilon = 1/2$, $z_2 = -2 = -\lambda$ the model is the usual 3D shell model and $H$ is the helicity as defined in Ref. [3]. By choosing $\lambda$ such that $\lambda = 1/(1-\epsilon)$, we get $E^2 = \Sigma(-1)^n\lambda^n|u_n|^2$. This form was argued in Ref. [3] to be the proper form for the helicity. In this paper we will alternatively use the definition (6) for the helicity.

For $\epsilon > 1$ the second conserved integral is positive definite and of the form

$$E^2 = Z = \frac{1}{2} \sum_{n=1}^{N} z_2^n |u_n|^2, \quad (7)$$

which can be interpreted as a generalized enstrophy. For $\epsilon = 5/4$, $z_2 = 4 = \lambda^2$ the model is the usual 2D shell model and $Z$ is the enstrophy as defined in Ref. [4]. The sign of $c$, which is the interaction coefficient for the smaller wave numbers, changes when going from the 3D to the 2D case. This could be related to the different role of backward cascading in the two cases. To see this, consider the nonlinear transfer of $E^i$ through the triad interaction between shells, $n-1, n, n+1$. This is simply given by

$$\dot{E}_{n-1}^i = k_{n-1}^{\alpha_i} \Delta_n,$$
$$\dot{E}_n^i = bz_i k_{n-1}^{\alpha_i} \Delta_n,$$
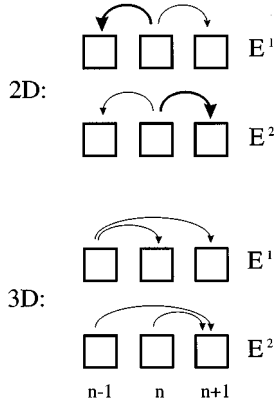$$\dot{E}_{n+1}^i = cz_i^2 k_{n-1}^{\alpha_i} \Delta_n, \quad (8)$$

with

FIG. 2. Shell triad interactions. Arrows indicate transfer of energy $E^1$ and enstrophy $E^2$ for the 2D case $\epsilon = 5/4$ and energy $E^1$ and helicity $E^2$ for the 3D case $\epsilon = 1/2$. The thickness of the arrows indicates the strength of the transfer.

$$\Delta_n = k_{n-1}\text{Im}(u_{n-1}u_n u_{n+1}). \qquad (9)$$

The detailed conservation of $E^i$ in the triad interaction is reflected in the identity $1 + bz_i + cz_i^2 = 0$; the exchange of energy $E^1$ with $\alpha_1 = 0$ is

$$\dot{E}_{n-1}^1 = \Delta_n,$$

$$\dot{E}_n^1 = -\epsilon \Delta_n,$$

$$\dot{E}_{n+1}^1 = (\epsilon - 1)\Delta_n \qquad (10)$$

and the exchange of helicity or enstrophy $E^2$ with $\alpha_2 = \alpha$ is

$$\dot{E}_{n-1}^2 = k_{n-1}^\alpha \Delta_n,$$

$$\dot{E}_n^2 = -[\epsilon/(\epsilon - 1)]k_{n-1}^\alpha \Delta_n,$$

$$\dot{E}_{n+1}^2 = [1/(\epsilon - 1)]k_{n-1}^\alpha \Delta_n. \qquad (11)$$

We have $\epsilon < 1$ for 3D-like models and $\epsilon > 1$ for 2D-like models. The two situations are depicted in Fig. 2, where the thickness of the arrows symbolizes the relative sizes of the exchanges in the cases of $\epsilon = 1/2$ and $\epsilon = 5/4$. The actual spectral transfer of $E^1$ and $E^2$ depends on the sign of $\Delta_n$; if $\Delta_n < 0$ all the arrows are turned around. If, on average, the transfer is as indicated in Fig. 2, there will be a transfer of energy and helicity from the large scales to the small scales in the 3D case and a transfer of enstrophy from the large to the small scales and a transfer of energy from the small scales to the large scales in the 2D case.

### B. Scaling and inertial range

The inertial subrange is defined as the range of shells where the forcing and the dissipation are negligible in comparison with the nonlinear interactions among shells. The spectrum of $E^{1,2}$ then, by the Kolmogorov hypothesis, depends only on $k$ and $\eta_{1,2}$, where $\eta_{1,2}$ is the time-averaged dissipation of $E^{1,2}$. From dimensional analysis we have $[ku] = s^{-1}$, $[\eta_{1,2}] = [E^{1,2}]s^{-1}$, and $[E^{1,2}] = [k^{\alpha_{1,2}}u^2] = [k]^{\alpha-2}s^{-2}$ and we get

$$E^{1,2} \sim \eta_{1,2}^{2/3} k^{(\alpha_{1,2}-2)/3}. \qquad (12)$$

For the generalized velocity, $u$, we then get the "Kolmogorov scaling"

$$|u| \sim \eta_{1,2}^{1/3} k^{-[\text{Re}(\alpha_{1,2})+1]/3}. \qquad (13)$$

The nonlinear cascade, or flux, of the conserved quantities defined by $z_{1,2}$ through shell number $n$ can be expressed directly as $\Pi_n^{1,2} = z_{1,2}^n(-\Delta_n/z_{2,1} + \Delta_{n+1})$. In the inertial range the cascade is constant $\Pi_n^{1,2} = \Pi_{n+1}^{1,2}$, so we get

$$z_1 z_2 \Delta_{n+2} - (z_1 + z_2)\Delta_{n+1} + \Delta_n = 0 \Rightarrow$$

$$z_1 z_2 (\lambda^{3\gamma+1})^2 - (z_1 + z_2)\lambda^{3\gamma+1} + 1 = 0, \qquad (14)$$

where we have assumed the scaling $u_n \sim k_n^\gamma \Rightarrow \Delta_n \sim k_n^{3\gamma+1}$. This gives the two solutions $\gamma_{1,2} = -(\alpha_{1,2}+1)/3$, which give for the cascade of $E^1$

$$\Pi^1 \sim \begin{cases} 1 - z_2/z_1 & \text{Kolmogorov for } E^1 \\ 0 & \text{fluxless for } E^1, \end{cases} \qquad (15)$$

and correspondingly for $E^2$,

$$\Pi^2 \sim \begin{cases} 0 & \text{fluxless for } E^2 \\ 1 - z_1/z_2 & \text{Kolmogorov for } E^2. \end{cases}$$

These are the two scaling fixed points for the model. The Kolmogorov fixed point for the first conserved integral corresponds to the fluxless fixed point for the other conserved integral and vice versa. This is of course just a reflection of the fact that (14) is symmetric in the indices 1 and 2. That these points in phase space are fixed points, in the case of no forcing and dissipation, is trivial, since $\Pi_n = \Pi_{n+1} \Rightarrow \dot{E}_{n+1} = 0 \Rightarrow \dot{u}_{n+1} = 0$. It should be noted that the Kolmogorov fixed point

$$u \sim k^{-(\alpha+1)/3} \qquad (16)$$

obtained from this analysis is in agreement with the dimensional analysis (12).

The scaling fixed points can be obtained directly from the dynamical equation as well. For $u_n \sim k_n^{-\gamma} = \lambda^{-n\gamma}$, we get by inserting into (1) with $a = 1$

$$\lambda^{n(1-2\gamma)-3\gamma}[1 + b\lambda^{3\gamma-1} + c(\lambda^{3\gamma-1})^2] = 0 \qquad (17)$$

and the generators reemerge $z_{1,2} = \lambda^{\alpha_{1,2}} = \lambda^{3\gamma_{1,2}-1}$, giving the Kolmogorov fixed points for the two conserved integrals $\gamma_{1,2} = (\alpha_{1,2}+1)/3$.

### III. FORWARD AND BACKWARD CASCADES

Until this point we have not specified which of the two conserved quantities will cascade. Assume, in the chaotic regime where the Kolmogorov fixed points are unstable, that there is, on average, an input of the same size of the two quantities $E^1$ and $E^2$ at the forcing scale; this can of course always be done by a simple rescaling of one of the quantities. If $N_d$ is a shell number at the beginning of the viscous subrange, we have that $u_{N_d}/k_{N_d} \approx \nu$ and the dissipation $D^i$ of
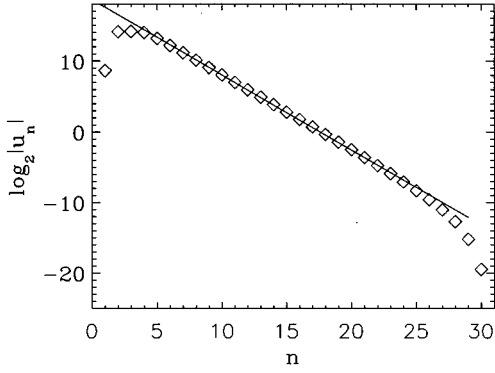
FIG. 3. Mean value of the shell velocities as a function of shell number on a logarithmic scale (base $\lambda$), for the 2D case $\epsilon = 5/4$, $k_0 = \lambda^{-4}$, $\lambda = 2$, $n = 30$, $\nu = 10^{-16}$, and $f_n = 5 \times 10^{-3} \times (1+i)\delta_{n,4}$. The model was run for $4.2 \times 10^4$ time units. The spectral slope, indicated by the line, is $-1.05$.

the conserved quantity, $E^i$ can be estimated as

$$D^i \sim \nu k_{N_d}^{\alpha_i + 2} |u_{N_d}|^2. \tag{18}$$

The ratio of dissipation of $E^1$ and $E^2$ scales with $k_{N_d}$ as $D^1/D^2 \sim k_{N_d}^{\alpha_1 - \alpha_2}$, so that, in the limit $Re \rightarrow \infty$ when $\alpha_1 < \alpha_2$, there will be no dissipation in the viscous subrange of $E^1$ where $E^2$ is dissipated. Therefore, a forward cascade
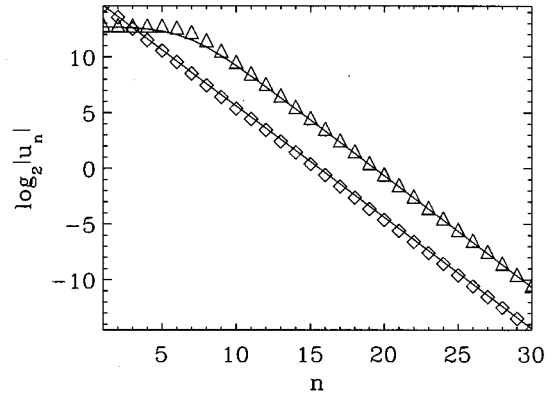


FIG. 5. Same as Fig. 3, but with $n = 30$ and $\nu = f = 0$. Diamonds correspond to an initial spectral slope of $-1.0$, which is a high value of $A/B$. The corresponding curve is the statistical equilibrium distribution for $A/B = 10^2$. Triangles corresponds to an initial spectral slope of $-0.8$, which is a lower value of $A/B$. The curve is the statistical equilibrium distribution for $A/B = 10^{-2}$.

of $E^1$ is prohibited and we should expect a forward cascade of $E^2$. For the backward cascade the situation is reversed, so we should expect a backward cascade of $E^1$.

The situation is completely different in the 2D-like and the 3D-like cases. In the 3D-like models $E^2$ is not positive definite, $E^2$ (helicity) is generated also in the viscous sub-
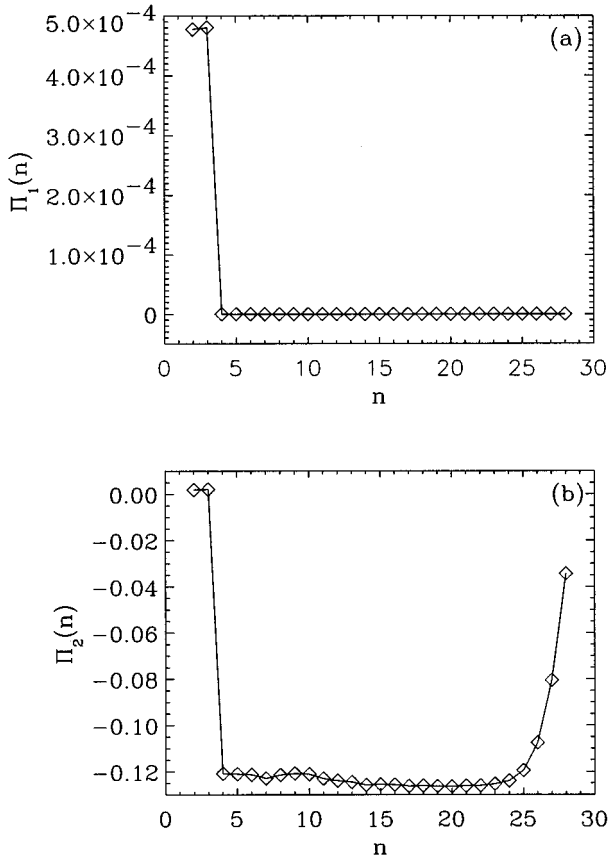


FIG. 4. Mean values of, (a) the energy flux $\Pi_1$ and (b) the enstrophy flux $\Pi_2$. The solid curves are guides for the eye.
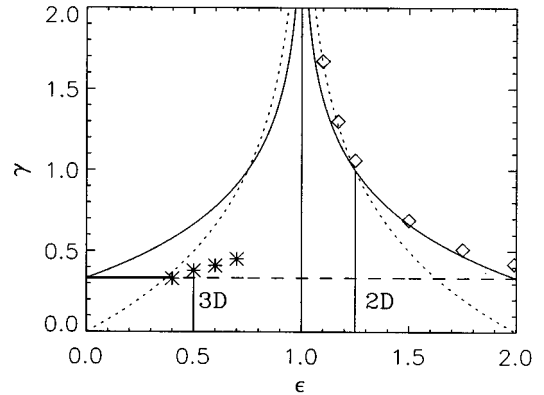


FIG. 6. Spectral slope $\gamma$ as a function of $\epsilon$. The horizontal dashed line is the Kolmogorov scaling for the energy cascade, the full curve is the scaling exponent for the enstrophy (or the 3D-like case of helicity) cascade, and the dotted curve corresponds to the enstrophy (helicity) equipartitioning. All the 3D-like models show an energy cascade (equipartitioning corresponds to the line $\gamma = 0$). The bold line segment, $0 < \epsilon < 0.39 \ldots$, represents parameter values where the Kolmogorov fixed point is stable [6]. The diamonds are a model run with $n = 50$, $k_0 = \lambda^{-4}$, $\lambda = 2$, $f_n = 5 \times 10^{-4} \times (1+i)\delta_{n,15}$, $(\epsilon = 11/10, \nu = 5 \times 10^{-27}, \nu' = 100)$, $(\epsilon = 117/100, \nu = 5 \times 10^{-27}, \nu' = 100)$, $(\epsilon = 5/4, \nu = 5 \times 10^{-25}, \nu' = 100)$, $(\epsilon = 3/2, \nu = 5 \times 10^{-21}, \nu' = 100)$, $(\epsilon = 7/4, \nu = 5 \times 10^{-21}, \nu' = 100)$, and $(\epsilon = 2, \nu = 5 \times 10^{-20}, \nu' = 100)$. The stars are model runs with $n = 19$, $k_0 = \lambda^{-4}$, $\lambda = 2$, $f_n = 10^{-4} \times (1+i)\delta_{n,4}$, $\nu = 10^{-6}$, and $\nu' = 0$, and $\epsilon = 1/2$, $6/10$, and $7/10$. The 3D-like models show Kolmogorov scaling, with deviations due to intermittency corrections, and energy cascading. The 2D-like models show a crossover at $\epsilon = 5/4$ between statistical equilibrium, $1 < \epsilon < 5/4$, and enstrophy cascading, $5/4 < \epsilon < 2$.
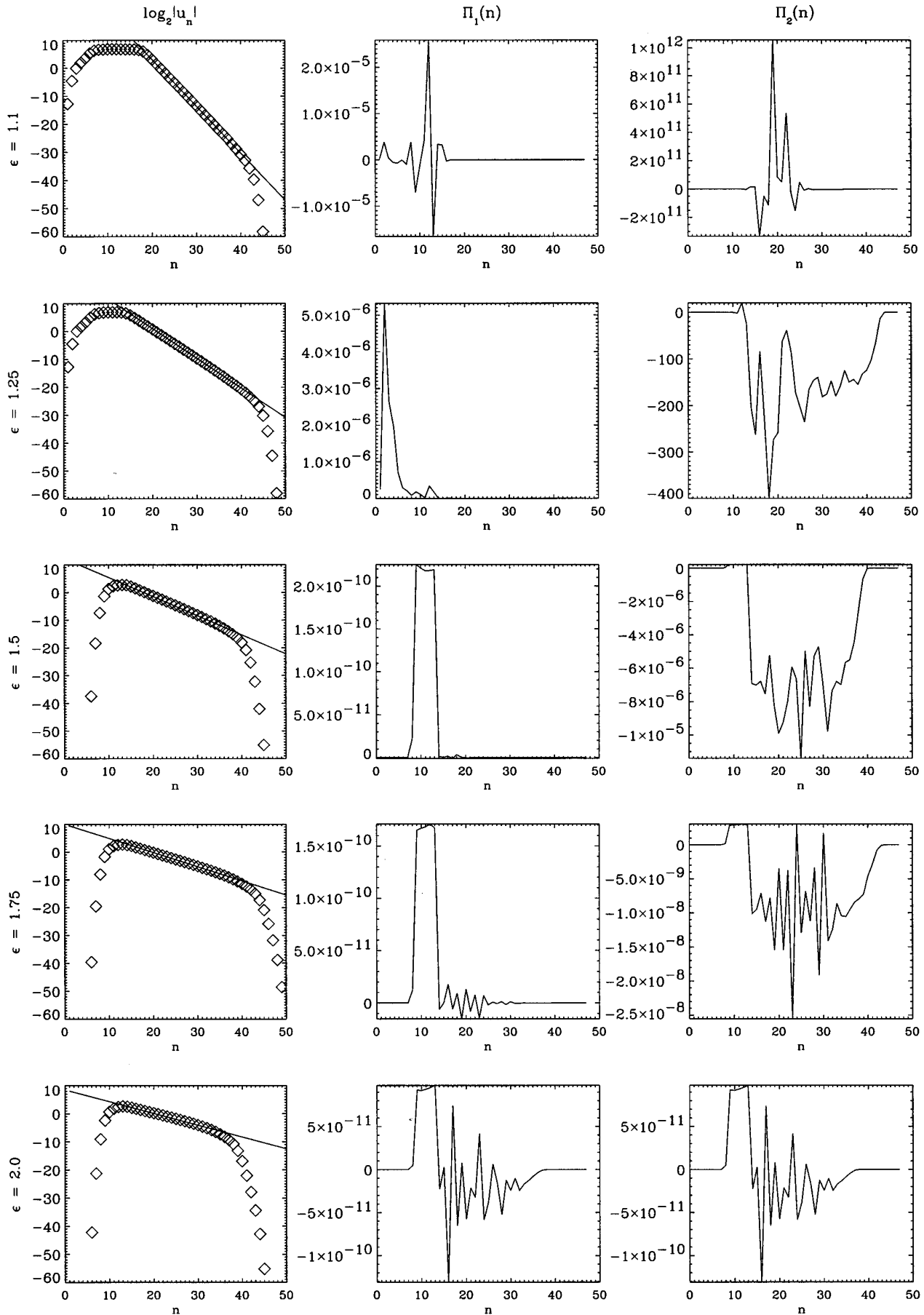
FIG. 7. Same as Figs. 3 and 4 for $\epsilon = 11/10$, 5/4, 3/2, 7/4, and 2. The spectral slopes, indicated by the lines, are shown in Fig. 6 (diamonds).
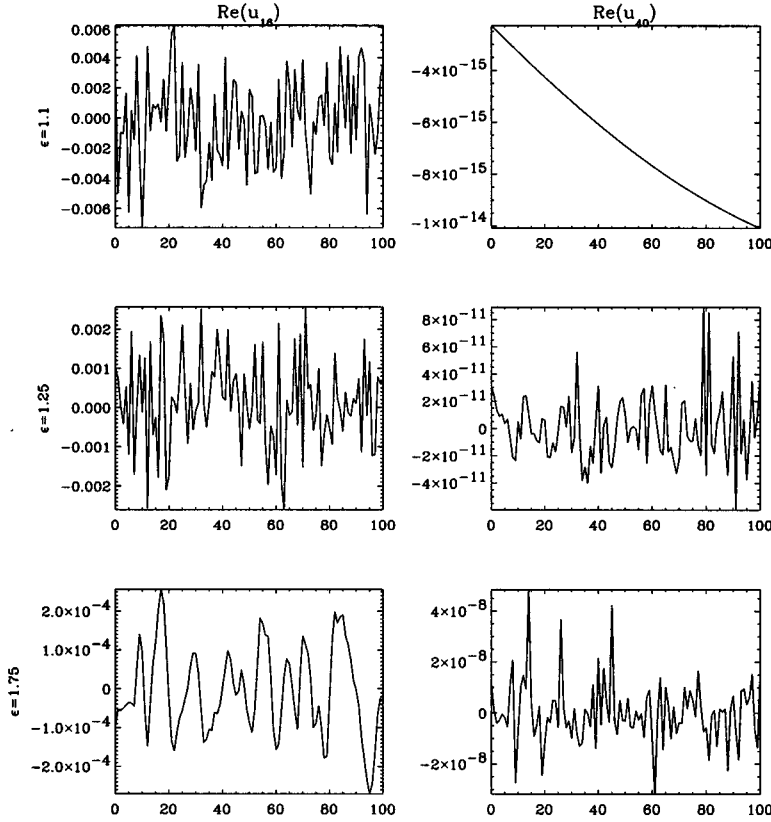
FIG. 8. Time evolution of shell velocities in the beginning and at the end of the inertial subrange. The typical time scale of shell $n$ scales as $T_n \sim (k_n|u_n|)^{-1} \sim k_n^{\gamma-1}$. Note that for $\epsilon = 5/4$ the time scale is the same for all shells.

range, and for the usual GOY model we do not see a forward cascade of helicity; see, however, Ref. [7]. This is in agreement with the observed $k^{-5/3}$ energy spectrum observed in real 3D turbulence corresponding to the forward cascade of energy. In the 2D case we observe the direct cascade of enstrophy, while the inverse cascade of energy is still debated. In the rest of this paper we will concentrate on 2D-like models where we will implicitly think of $E^1 = E$, with $\alpha_1 = 0$, as the energy and $E^2 = Z$, with $\alpha_2 = \alpha > 0$, as the enstrophy. With regard to the inverse cascade of energy one must bear in mind that in 2D turbulence the dynamics involved is probably related to the generation of large scale coherent structures, vortices, and vortex interactions. Vortices are localized spatially, thus delocalized in spectral space. This is in agreement with the estimate that 2D is marginally delocalized in spectral space [8]. In the GOY model there is no spatial structure and the interactions are local in spectral space. The model is therefore probably not capable of showing a realistic inverse energy cascade. We will thus only consider the forward cascade in this paper. Figure 3 shows the scaling in the inertial subrange of the model with $\epsilon = 5/4$ corresponding to $\alpha = 2$. The cascades of the enstrophy and energy are shown in Fig. 4. It is seen that enstrophy is forward cascaded while energy is not.

## IV. STATISTICAL DESCRIPTION OF THE MODEL

In a statistical equilibrium of an ergodic dynamical system we will have a probability distribution among the (finite) degrees of freedom, assuming an ultraviolet cutoff, of the form $P_i \sim \exp(-BE_i^1 - AE_i^2)$, where $E^1$ and $E^2$ are the conserved quantities, energy and enstrophy. Thus the temporal mean of any quantity, which is a function of the shell velocities, is given as

$$\bar{g} = \int \prod_i du_i\, g(u_1, \ldots, u_N) \exp(-BE_i^1 - AE_i^2) \Big/ \int \prod_i du_i \exp(-BE_i^1 - AE_i^2). \qquad (19)$$

$A$ and $B$ are Lagrange multipliers, reflecting the conservation of energy and enstrophy when maximizing the entropy of the system, corresponding to inverse temperatures, denoted as inverse ''energy'' and ''enstrophy temperatures'' [9].

The shell velocities themselves will in this description be independent and Gaussian distributed variables with standard deviation $\sigma(u_i) = 1/[2(Bk_i^{\alpha_1} + Ak_i^{\alpha_2})]$. The average values of the energy and enstrophy becomes

$$2\bar{E}^{-1}_{i} = k^{\alpha_1}_i |\bar{u}^{-}_i|^2 = (B + A k^{\alpha_2 - \alpha_1}_i)^{-1},$$

$$2\bar{E}^{-2}_{i} = k^{\alpha_2}_i |\bar{u}^{-}_i|^2 = (B k^{\alpha_1 - \alpha_2}_i + A)^{-1}. \qquad (20)$$

For $k \to 0$ we will have equipartitioning of energy $k^{\alpha_1}_i |\bar{u}^{-}_i|^2 = B^{-1}$ and the scaling $|u_i| \sim k^{-\alpha_1/2}_i$ and for the other branch $k \to \infty$ we will have equipartitioning of enstrophy $k^{\alpha_2}_i |\bar{u}^{-}_i|^2 = A^{-1}$ and the scaling $|u_i| \sim k^{-\alpha_2/2}_i$. In the case of no forcing and no viscosity the equilibrium will depend on the ratio $A/B$ between the initial temperatures $A^{-1}, B^{-1}$. To illustrate this we ran the model without forcing and viscosity but with two different initial spectral slopes of the velocity fields, the larger the slope the higher the ratio of the energy temperature to the enstrophy temperature. Figure 5 shows the equilibrium spectra for $\epsilon = 5/4, \nu = f = 0$, in the cases of initial slopes $-1, -0.8$. The full lines are the equilibrium distribution given by (20) for $A/B = 10^2$ and $A/B = 10^{-2}$, respectively.

## V. DISTINGUISHING CASCADE FROM STATISTICAL EQUILIBRIUM

For the forward enstrophy cascade the spectral slope is $-(\alpha + 1)/3$ and the enstrophy equipartitioning branch has
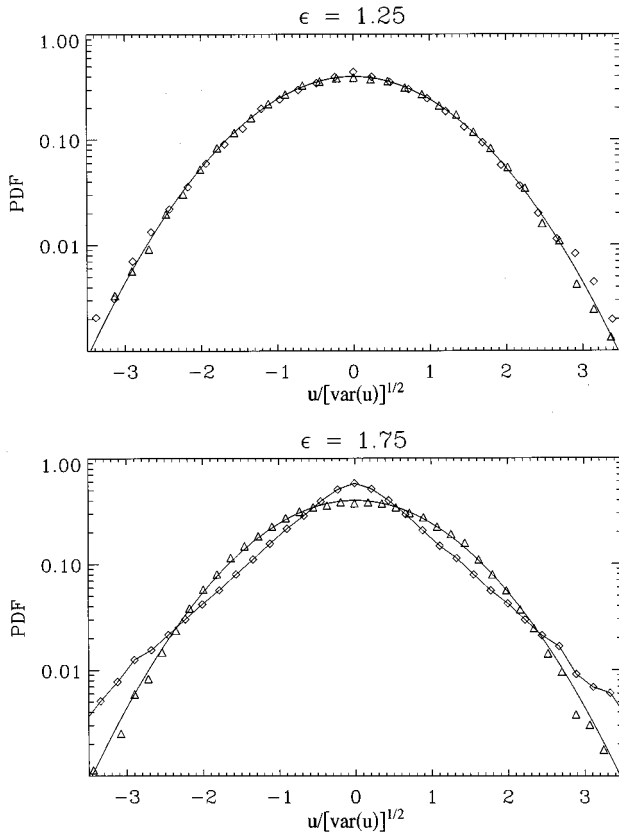


FIG. 9. Probability density functions for real part of the shell velocities of shells 18 (triangles) and 40 (squares). The parabolas are Gaussians with the same variance. The upper panel shows the PDF's for $\epsilon = 5/4$ with Gaussians at both ends of the inertial range. The lower panel shows the PDF's for $\epsilon = 7/4$ with a Gaussian in the beginning of the inertial range and a distribution towards a Laplacian at the end of the inertial range, corresponding to an intermittent signal. The second curve is a guide for the eye.

spectral slope $-\alpha/2$. Thus, for the 2D case where $\alpha = 2$ we cannot distinguish between statistical (quasi)equilibrium and cascading. This was pointed out by Aurell et al. [4] and it was argued that the model can be described as being in statistical quasiequilibrium with the enstrophy transfer described as a simple diffusion rather than an enstrophy cascade. This coinciding scaling is a caviate of the GOY model not present in the real 2D flow where the statistical equilibrium energy spectrum scales as $k^{-1}$ and the cascade energy spectrum scales as $k^{-3}$. For other values of $\alpha$ the scaling of the two cases are different, see Fig. 6. This figure represents the main message of this paper. The first axis is the parameter $\epsilon$, along the line shown in Fig. 1, defining the spectral ratio between the two inviscid invariants. The second axis is the scaling exponent $\gamma$. The horizontal dashed line $\gamma = 1/3$ is the Kolmogorov scaling exponent for energy cascade. The full curve is the scaling exponent for the enstrophy cascade and the dotted curve corresponds to the enstrophy equipartitioning.

All the 3D-like models (asterisks in Fig. 6) are near energy cascade scaling (dashed line). Statistical equilibrium corresponds to the line $\gamma = 0$. The bold line segment $0 < \epsilon < 0.39 \ldots$ represents parameter values where the Kolmogorov fixed point is stable [6]. The scaling for $\epsilon > 0.39 \ldots$ is slightly steeper than the Kolmogorov scaling, which is attributed to intermittency corrections originating from the viscous dissipation [10]. It seems as if there is a slight trend showing increasing spectral slopes for increasing $\epsilon$.

For the 2D-like models the scaling slope is also everywhere on or slightly above both the cascade and the equilibrium slopes (diamonds in the figure). The classical argument for a cascade is that given an initial state with enstrophy concentrated at the low-wave-number end of the spectrum, the enstrophy will flow into the high wave numbers in order to establish statistical equilibrium. The ultraviolet catastrophe is then prevented by the dissipation in the viscous subrange. Therefore, we cannot have a nonequilibrium distribution with more enstrophy in the high-wave-number part of the spectrum than prescribed by statistical equilibrium since enstrophy in that case would flow from high to low wave numbers. This means that the spectral slope in the inertial subrange always is above the slope corresponding to equilibrium (dotted line in Fig. 6). Consequently, the 2D model with $\epsilon = 5/4$ separates two regimes: $1 < \epsilon < 5/4$, where enstrophy equilibrium is achieved, and $5/4 < \epsilon < 2$, where the enstrophy is cascaded through the inertial range.

In Fig. 7 the spectra and the cascades are shown for different values of $\epsilon$. The model was run with 50 shells and forcing on shell number 15 for $2 \times 10^4$ time units and averaged. Even then there are large fluctuations in the cascades not reflected in the spectra. The large differences in the absolute values for the cascades $\pi$ is a reflection of the scaling relation (18).

We interpret the peaks around the forcing scale for $\epsilon = 11/10$ as statistical fluctuation and the model shows no cascade. For $\epsilon > 5/4$ we see an enstrophy cascade and what seems to be an inverse energy cascade. However, we must stress that we do not see a second scaling regime for small $n$ corresponding the inverse cascade. Note that for $\epsilon = 2$ energy and enstrophy are identical and we have only one invis-
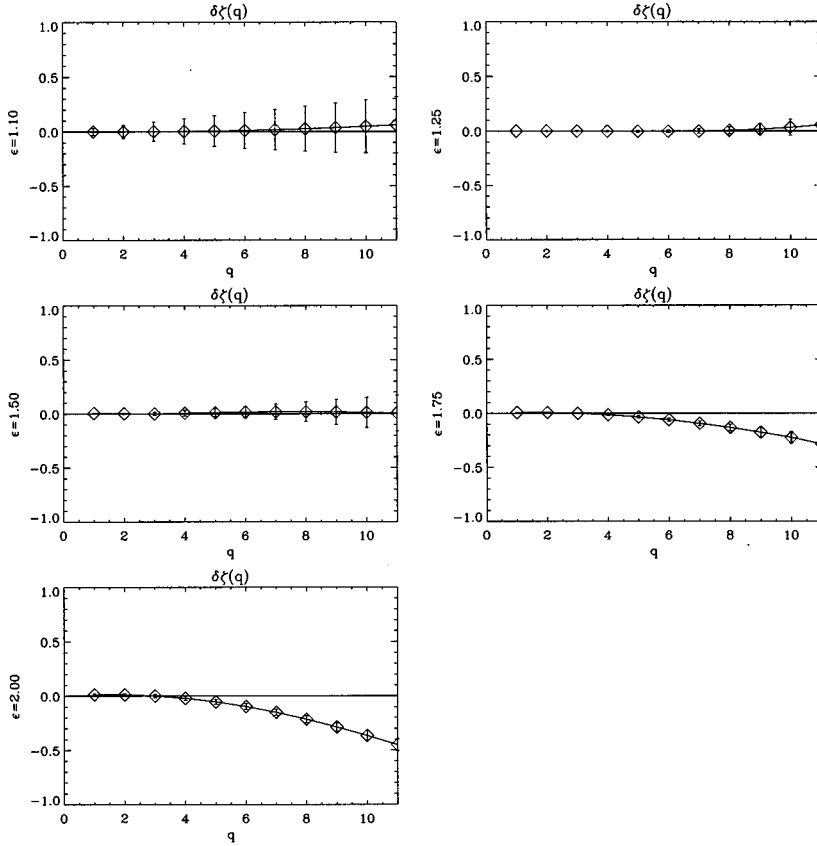
FIG. 10. Deviation of the structure function from Kolmogorov scaling for $\epsilon = 11/10$, 5/4, 3/2, 7/4, and 2.

cid invariant. So if a regime of inverse energy cascading existed in parameter space near $\epsilon = 2$ the scaling exponents would be almost identical and coincide at $\epsilon = 2$.

The two regimes corresponding to equipartitioning and cascade can be understood in terms of time scales for the dynamics of the shell velocities. A rough estimate of the time scales for a given shell $n$ is, from (1), given as $T_n \sim (k_n u_n)^{-1} \sim k_n^{\gamma - 1}$. Again $\epsilon = 5/4$, corresponding to $\gamma = 1$, becomes marginal where the time scale is independent of shell number. For $\epsilon < 5/4$ the time scale grows with $n$ and the fast time scales for small $n$ can equilibrate enstrophy among the degrees of freedom of the system before the dissipation, at the ''slow'' shells, has time to be active. Therefore these models exhibit statistical equilibrium. For $\epsilon > 5/4$ the situation is reversed and the models exhibit enstrophy cascades. Time evolutions of the shell velocities are shown in Fig. 8, where the left columns show the evolution of a shell in the beginning of the inertial subrange and the right columns show the evolution of a shell at the end of the inertial subrange. This time-scale scaling might also explain why no inverse cascade branch has been seen in the GOY model. The time-scales at the small-wave-number end of the spectrum, with the dissipation or drag range for inverse cascade, is long in comparison with the time scales of the inertial range of inverse cascade. Therefore a statistical equilibrium will have time to form. The analysis suggests that parameter choices $\epsilon > 5/4$ might be more realistic than $\epsilon = 5/4$ for mimicking enstrophy cascade in real 2D turbulence.

## VI. INTERMITTENCY CORRECTIONS

The numerical result that the inertial range scaling has a slope slightly higher than the Kolmogorov 1941 prediction is not fully understood. This is attributed to intermittency corrections originating from the dissipation of enstrophy in the viscous subrange.

The evolution of the shell velocities in the viscous subrange is intermittent for $\epsilon > 5/4$, where the probability density functions (PDF's) are non-Gaussian, while the PDF's for $\epsilon = 5/4$ are Gaussian in both ends of the inertial subrange; see Fig. 9. The deviation from the Kolmogorov scaling is expressed through the structure function $\zeta(q)$ [10]. The structure function is defined through the scaling of the moments of the shell velocities

$$|\bar{u}_n|^q \sim k_n^{\zeta(q)} = k_n^{-q\gamma - \delta\zeta(q)}, \quad (21)$$

where $\delta\zeta(q)$ is the deviation from Kolmogorov scaling. The structure function $\zeta(q)$ and $\delta\zeta(q)$ for $\epsilon = 11/10$, 5/4, 3/2, 7/4, and 2 are shown in Fig. 10. For $\epsilon > 5/4$ there are intermittency corrections to the scaling in agreement with what the PDF's show. In calculating the structure function the poor statistics reflected in the noisy PDF's are compensated by having a rather large number of shells, of the order 20, in the inertial range.

We know of no analytic way to predict the intermittency corrections from the dynamical equation. Our numerical calculations suggest that the intermittency corrections are con-
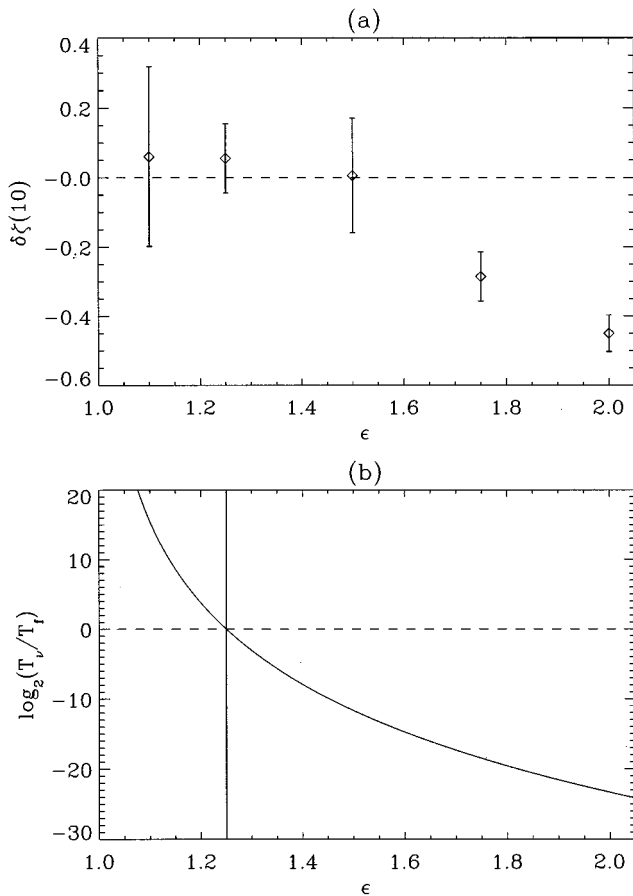
FIG. 11. (a) Numerical values of $\delta\zeta(10)$ as a function of $\epsilon$. The error bars represent one standard deviation. (b) Ratio of typical time scales between the dissipation scale and the forcing scale. $\log_2(T_\nu/T_f)$ is a function of $\epsilon$. The vertical line indicates the crossover between statistical equilibrium and cascading.

nected with the differences in typical time scales from the beginning of the inertial subrange, where the model is forced, to the viscous subrange. The ratio of time scales between the dissipation scale and the forcing scale can be estimated by $T_\nu/T_f \approx \lambda^{\Delta N(\gamma-1)}$, where $\Delta N$ is the number of shells between the two. Figure 11(a) shows the numerical values of $\delta\zeta(10)$ as a function of $\epsilon$ and Figure 11 (b) shows $\log_2(T_\nu/T_f)$ as a function of $\epsilon$. The vertical line indicates the crossover between statistical equilibrium and cascading.

We must stress that caution should be taken upon drawing conclusions from this since the authors have no physical explanation of the apparent relationship.

## VII. SUMMARY

The GOY shell model has two inviscid invariants, which govern the behavior of the model. In the 2D-like case these corresponds to the energy and the enstrophy of 2D turbulent flow. In the model we can change the interaction coefficient $\epsilon$ and tune the spectral ratio of enstrophy to energy $Z_n/E_n = k_n^\alpha$. For $\alpha > 2$ we can describe the dynamics as being in statistical equilibrium with two scaling regimes corresponding to equipartitioning of energy and enstrophy, respectively. The reason for the equipartitioning of enstrophy in the inertial range (of forward cascading of enstrophy) is that the typical time scales, corresponding to eddy turnover times, are growing with shell number, thus the time scale of viscous dissipation is large in comparison with the time scales of nonlinear transfer. Thus this choice of interaction coefficient is completely unrealistic for mimicking cascades in 2D turbulence. For $\alpha < 2$ the model shows forward cascading of enstrophy, but we have not identified a backward cascade of energy. The usual choice $\epsilon = 5/4$, $\alpha = 2$ is a borderline and we suggest that $\alpha < 2$ in respect to mimicking enstrophy cascade might be more realistic. We observe that the dynamics becomes more intermittent when $\alpha < 2$, in the sense that the structure function deviates more and more from the Kolmogorov prediction. For $\epsilon = 2$ we have $\alpha = 0$, thus energy and enstrophy degenerate into only one inviscid invariant; this point could then be interpreted as a model of 3D turbulence. However, as is seen from (15), in this case the fluxless fixed point is the one surviving, but as seen in Fig. 7, bottom panels, this model also shows cascading. This choice for 3D turbulence model could shed some light on the dispute of the second inviscid invariant (helicity) being important [3] or not [11] for the deviations from Kolmogorov theory. Work is in progress on this point.

*Note added:* The authors have recently become aware of related work for a slightly different set of GOY models in M. Yamada and K. Ohkitani, Phys. Lett. A **134**, 165 (1988).

[1] E. B. Gledzer, Dokl. Akad. Nauk SSSR **18**, 216 (1973) [Sov. Phys. Dokl. **18**, 216 (1973)].

[2] M. Yamada and K. Okhitani, J. Phys. Soc. Jpn. **56**, 4210 (1987); Prog. Theor. Phys. **79**, 1265 (1988); Phys. Rev. Lett. **60**, 983 (1988).

[3] L. Kadanoff, D. Lohse, J. Wang, and R. Benzi, Phys. Fluids **7**, 617 (1995).

[4] E. Aurell, G. Boffetta, A. Crisanti, P. Frick, G. Paladin, and A. Vulpiani, Phys. Rev. E **50**, 4705 (1994).

[5] P. Frick and E. Aurell, Europhys. Lett. **24**, 725 (1993).

[6] L. Biferale, A. Lambert, R. Lima, and G. Paladin, Physica D **80**, 105 (1995).

[7] P. D. Ditlevsen, Phys. Rev. E (to be published).

[8] R. H. Kraichnan and D. Montgomery, Rep. Prog. Phys. **43**, 547 (1980).

[9] R. H. Kraichnan, J. Fluid Mech. **47**, 525 (1971).

[10] M. H. Jensen, G. Paladin, and A. Vulpiani, Phys. Rev. A **43**, 798 (1991).

[11] O. Gat, I. Procaccia, and R. Zeitak, Phys. Rev. E **51**, 1148 (1995).